PHYSICAL REVIEW B, VOLUME 64, 195101

Effect of structural disorder on the Urbach energy in Cu ternaries

S. M. Wasim, C. Rincón, G. Marín, and P. Bocaranda
Centro de Estudios de Semiconductores, Facultad de Ciencias, Universidad de Los Andes, Mérida 5101, Venezuela

E. Hernández
Departamento de Física, Facultad Experimental de Ciencias, Universidad del Zulia, Maracaibo, Venezuela

Ismardo Bonalde and Ernesto Medina
Centro de Física, IVIC, Apartado 21827, Caracas 1020-A, Venezuela

(Received 31 January 2001; published 12 October 2001)

From the analysis of the Urbach tail in $CuInSe_2$ and $CuInTe_2$, it is found that the energy $h\nu_p$ involved in the electron−exciton-phonon interaction is not that of the ordered compound longitudinal or transverse optical modes. It is established that this energy depends on the structural and cations disorders. An expression of the form $E_U(T,P,N)=K\Theta/\sigma_0\{(1+P)/2+N[\exp(\Theta/T)-1]^{-1}\}$, where P and N are adjustable structural and order-disorder parameters and Θ the Einstein characteristic temperature, accurately explains the temperature dependence of the Urbach energy. From extrapolation of the linear variation of N and P with $h\nu_p$, the phonon energy for a completely ordered and disordered systems can be estimated. We discuss the physical meaning of the parameter N as due to the contribution of localized modes produced by substitutional disorder of low energy of formation. We find an intriguing relation between the temperature of the chalcopyrite-sphalerite transition and the phonons contributing to the formation of Urbach tails in the strong-disorder limit.

DOI: 10.1103/PhysRevB.64.195101 PACS number(s): 71.35.Cc, 78.20.Ci, 78.30.Ly

I. INTRODUCTION

The optical absorption coefficient α just below the band edge in insulators and semiconductors is found to vary exponentially with the incident photon energy. This dependence of α, first observed by Urbach[1] in indirect-gap silver halides and by Martienssen[2] in direct-gap alkalide halides, is referred to in the literature as the Urbach-Martienssen or simply Urbach rule. It is found that, at a given temperature, α follows the relation[3]

$$\alpha=\alpha_0\exp[\sigma(h\nu-E_0)/KT], \tag{1}$$

where α_0 and E_0 are characteristic parameters of the material, σ the steepness parameter, $h\nu$ the incident photon energy, and T the temperature. This implies that a plot of $\ln\alpha$ against $h\nu$ near the band edge can be represented by a straight line. The extrapolation of these lines corresponding to different temperatures tends to converge at a point defined by α_0 and E_0 in Eq. (1). The parameter E_0, also called the converging energy, is necessarily higher than the optical band gap energy. The relation KT/σ, which is the width of the exponential tail, is called the Urbach energy E_U. Because of the nature of the temperature dependence of the Urbach tail, Sumi and Toyozawa[4] suggested that the exponential behavior of α originates from the interaction of electrons and excitons with phonons.[5]

Exciton-phonon interactions are of much interest in relation to the photon absorption characteristic of solar cell materials. In such materials there is an interplay between the efficiency of energy capture and the resulting material resistance. The presence of disorder and thermal fluctuations reduces the gap by means of band tails but, on the other hand, increases carrier scattering. As discussed here, Urbach tails can be a telltale signature of the presence of different types of impurities and disorder. Recent works have studied Urbach tails in association with energy distortions caused by compositional disorder in $CuIn_3Se_5$ and $CuGa_3Se_5$,[6] impurity binding energies in amorphous silicon,[7,8] and probe order-disorder transitions in ferroelectric material.[9] In particular, we will show the signals of the chalcopyrite-sphalerite order-disorder transition through the behavior of Urbach tails. Finally, Urbach tails and the photon absorption spectra give information about the exciton dynamics,[5] distinguishing between free and trapped excitons in the lattice.

The steepness parameter σ in Eq. (1) has been found to follow the relation[4]

$$\sigma=\sigma_0\frac{2KT}{h\nu_p}\tanh\left(\frac{h\nu_p}{2KT}\right), \tag{2}$$

where σ_0 is a constant independent of temperature, and $h\nu_p$ corresponds to the energy of phonons associated with the Urbach tails. Equation (2) corresponds theoretically to the thermal average over potential fluctuations of a harmonic lattice in the dispersionless approximation with linear exciton-phonon interactions.[5] Within such theory, σ_0 is inversely proportional to the exciton-phonon interaction strength. The energy $h\nu_p$ is suggested to be the energy of phonons involved in the formation of the photon absorption edge. This phonon energy, in general, is found to be in the same range as the lattice vibrational modes. Hence, depending on the proximity of the experimental value of $h\nu_p$ to one of the vibrational modes, it is believed that the Urbach tail originates from an exciton-phonon interaction that involves a transverse acoustical (TA) mode in CdS, transverse optical (TO) mode in CdSe, longitudinal acoustical (LA) mode in ZnS, and both LO and TO modes in CdTe, ZnTe, and ZnSe.[3]

Several values of $h\nu_p$ appreciably larger than the energy corresponding to the highest optical mode and that differ from one sample to another of the same material have been reported[3] in II-VI zin-cblende semiconductors. It has been argued that the higher energy values could be due to the high crystal symmetry in such systems.[3,10] However, similar behavior has also been observed in $CuInSe_2$ (CIS),[10,11] $CuInTe_2$(CIT),[12] $CuIn_3Se_5$,[13] and $CuGa_3Se_5$.[14] These compounds belong to the I-III-VI_2 family of chalcopyrite semiconductors which are the derivatives of II-VI compounds and hence have lower symmetry.

On the other hand, E_U is expected to be a direct measure of the temperature-induced disorder and reflects the thermal occupancy of phonon states in the crystal.[4,15] From the standard treatment of Urbach tails in crystalline semiconductors, it is then concluded that KT/σ is proportional to the thermal average $\langle U^2\rangle_T$. This thermal average, like the Debye-Waller factor, is a measure of the square of the displacement U of the atoms from their equilibrium position.

To compare the experimental Urbach energy with a theoretical model, Cody *et al.*[15] proposed an empirical relation that takes into account both the interaction of electrons and excitons with phonons and the static structural disorder, especially in amorphous semiconductors. This concept has also been extended to mixed binary and ternary compounds[10] with limited success. Cody *et al.*[15] introduced, in addition to $\langle U^2\rangle_T$, an extra term $\langle U^2\rangle_X=(\Theta/\sigma_0)(X/2)$ in Eq. (2) where $\langle U^2\rangle_X$ is the contribution of structural (topological) disorder to the mean-square deviation of atomic positions beyond those of zero-point fluctuations.[15] Θ is the Einstein temperature, related to the Debye temperature by $\Theta\sim 3/4\Theta_D$. Under these considerations the proposed expression for E_U takes the form

$$E_U(T,X)=\frac{K\Theta}{\sigma_0}\left(\frac{1+X}{2}+\frac{1}{\exp(\Theta/T)-1}\right). \tag{3}$$

Although the E_U versus T data of Cody *et al.* on α-Si:H could be explained quite successfully with Eq. (3), we will show that the variation of E_U with T in $CuInSe_2$, $CuInTe_2$, $CuIn_3Se_5$, and $CuGa_3Se_5$ cannot be fitted satisfactorily using X as an adjustable parameter.[10] The disagreement is not surprising since the physical nature of topological disorder in amorphous semiconductors is expected to be quite different from the structural defects produced by cation-cation disorder and the deviation from the ideal stoichiometry 1:1:2 and 1:3:5 in I-III-VI_2 and I-III_3-VI_5 compounds, respectively. Thus, from what has been described so far, it is evident that the models proposed to explain Urbach tails in elemental semiconductors do not offer the complete picture as far as the binary and especially the ternary compound semiconductors are concerned. This is reflected in (a) the unexplained high values of the phonon energy involved in the formation of the absorption edge and (b) the shortcoming of the topological disorder model to account for the variation of the Urbach energy with temperature.

Hence, to understand and establish the importance of the physics of structural defects caused by cation-cation disorder and deviation from the ideal stoichiometry on the Urbach tails, in the present work we report a systematic study of the optical absorption edge in several single-crystal samples of known stoichiometry of $CuInSe_2$ at different temperatures. Data published by Shioda *et al.*[10] and Nakanishi *et al.*[16] and other results published earlier by the authors[12] are also analyzed. We find a linear correlation between the phonon mode energies $h\nu_p$ and newly defined parameters that incorporate the deviations from ideal cation-cation and anion-cation ratios. The high values of $h\nu_p$ can be explained as originating from the contribution of the additional phonon energy due to structural defects. An empirical relation is proposed that accurately accounts for the variation of E_U with T in all the samples. Analysis of the parameters in such expression leads to important conclusions.

II. EXPERIMENTAL METHODS

Single crystals of CIS were grown by a technique[17] that consists of the selenization in liquid phase of stoichiometric proportions of Cu and In and later solidification under programmed varying gradient in a fully automated multiple zone horizontal furnace. By this method, several ingots were grown by varying the evaporation temperature of Se from 450 to 800 °C. Samples cut from the middle region of the ingots grown with evaporation temperature at 650, 700, and 750 °C and others grown by the standard vertical Bridgman technique are termed CIS650, CIS700, CIS750, and CIS40. $CuInTe_2$ samples were obtained from a similar tellurization technique reported elsewhere.[18]

The stoichiometric composition of the samples was determined at several points by energy dispersive x-ray spectroscopy using a Kevex Model Delta-3 system connected to a Hitachi model S-2500 scanning electron microscope. The error in the standard analysis was around ±5%. No significant variation in the composition from one part of the sample to another confirmed its homogeneity. The chalcopyrite structure was confirmed by x-ray diffraction study.

The optical absorption coefficient α at different temperatures between 10 and 300 K was obtained with a fully automated Cary 17I spectrophotometer using a tungsten lamp as a light source.[19] An Air Products cryostat cooled by helium gas was used to obtain the spectra. The transmitted radiation was detected by a Ge photodiode connected to a PAR model 5208 lock-in amplifier.

The absorption coefficient spectra α was obtained through the relation

$$\alpha=(1/t)[2\ln(1-R)-\ln(T-T_m)]-\alpha_0, \tag{4}$$

where t is the thickness of the sample, R the reflectance, and T the transmittance. T_M and α_0 are included in Eq. (4) to subtract the nearly constant apparent transmittance induced by diffused stray light in the high-energy side of the spectra and the nearly constant background absorption observed in the low-energy range, respectively. R was taken as 0.256 for CIT (Ref. 20) and 0.250 for CIS (Ref. 21).

III. EXPERIMENTAL RESULTS AND DISCUSSION

The logarithmic variation of α with photon energy $h\nu$, just below the fundamental absorption edge at several tem-

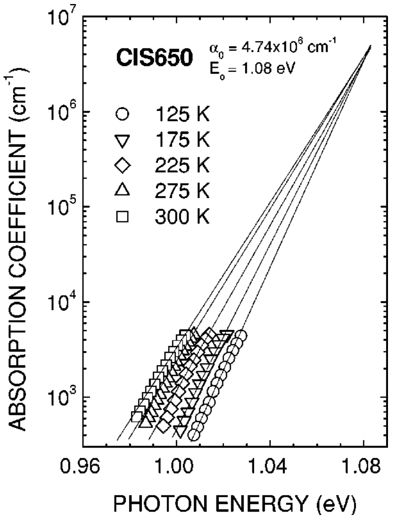

FIG. 1. Logarithmic variation of the absorption coeficient α with the photon energy $h\nu$ at several temperatures between 125 and 300 K, just below the fundamental absorption edge, for a representative sample CIS650 of $CuInSe_2$.

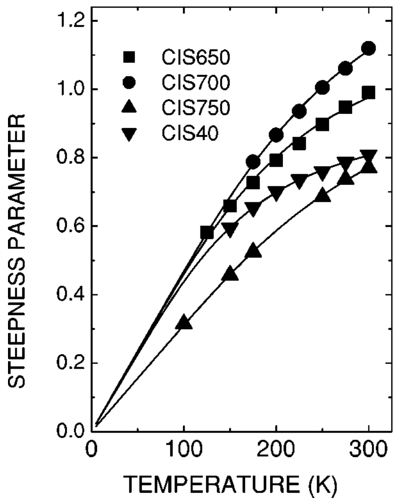

FIG. 2. The steepness parameter σ as a function of temperature for $CuInSe_2$ samples CIS650 (squares), CIS700 (circles), CIS750 (triangles), and CIS40 (inverted triangle). The solid curves represent a fit to Eq. (2) with the adjustable parameters σ_0 and $h\nu_p$ given in Table I.

peratures between 100 and 300 K, is shown in Fig. 1 for a representative sample CIS650 of $CuInSe_2$. To maintain the clarity of the figure, a ln α versus $h\nu$ plot is given for limited number of temperatures. A linear dependence is observed within a certain energy range up to one order of magnitude in α at each temperature in CIS650 and other samples (not shown here). In agreement with Urbach's rule, the extrapolation of the fitted continuous lines in this range of α converges to a single point. The corresponding values of α_0 and E_0 at the converging point for the four samples studied in the present work and some of those reported by Shioda *et al.*[10] and Nakanishi *et al.*[16] are given in Table I. An E_0 slightly higher than the energy gap is consistent with that reported for the other semiconductors. The magnitude of α_0 and E_0 in the present work, and those of Refs. 12 and 16, vary somewhat within 0.02 eV from one sample to another.

TABLE I. The parameters E_0 (eV) and α_0 (cm^{-1}) associated with Urbach tails in $CuInSe_2$ samples of the present work, those reported in Refs. 10,16, and also of $CuInTe_2$, of Ref. 12.

Samples	E_0 (eV)	α_0 (10^6 cm^{-1})
CIS40[a]	1.06	0.07
CIS650[a]	1.08	4.74
CIS700[a]	1.08	8.96
CIS750[a]	1.06	1.41
CIS6 (Fig. 1)[b]	1.08	2.0
CIS9 (Fig. 3)[c]	1.04	0.08
CIS10 (Fig. 3)[c]	1.07	3.6
S530[d]	1.03	2.8
S590[d]	1.08	2.6
S690[d]	1.08	2.5
STVB[d]	1.04	2.7

[a] Present work.
[b] Figure 1 in Ref. 10.
[c] Figure 3 of Ref. 16.
[d] Reference 12.

σ is calculated from the slope of the fitted Urbach tail represented by Eq. (1). These values are plotted in Fig. 2 as a function of temperature for all the CIS samples studied by us. To get an estimate of the phonon energy associated with the Urbach tail, the data in Fig. 2 are fitted to Eq. (2) with σ_0 and $h\nu_p$ as adjustable parameters. The values of σ_0 and $h\nu_p$, thus obtained, for different samples and those interpolated from Fig. 6 of Ref. 10 and Fig. 3 of Ref. 16 are given in Table II.

It is well known that CIT and CIS have a tetragonal space group $I\bar{4}2d$, and there are expected to be 21 optical and 3 acoustic vibrational modes. Of these, Tanino *et al.*[22] have reported 13 modes at room temperature and 22 at 100 K in CIS. The energy of these modes varies from the lowest at 7 meV to the highest value at 29 meV. However, all the $h\nu_p$ values obtained from the fit to the data with Eq. (2) in the present work and in Refs. 10 and 16 are larger than the phonon energies of these modes. For example, the smallest value of $h\nu_p = 35$ meV observed in CIS40 is higher than the highest phonon energy of the LO mode which is 29 meV. Large values of $h\nu_p$ between 37 and 56 meV by Shioda *et al.*, between 35 and 57 meV by Nakanishi *et al.*, and 71.2 meV by Medvedkin *et al.*[23] have also been reported for this compound. On the other hand, the reported energies of phonon modes in CIT are between 6 and 23 meV, as obtained from infrared reflectivity measurements[24] and through the analysis of the phonon spectra,[25] whereas those observed from a fit to the σ versus T data lie between 20 and 33 meV. Furthermore, $h\nu_p$ between 58 and 68 meV, estimated in several samples of the ordered vacancy compound $CuIn_3Se_5$,[13] is much higher than the energy of its highest reported optical mode of 27 meV.[26] Similar is the case for $CuGa_3Se_5$, where $h\nu_p$ is 60 meV, almost double its highest reported mode.[26] These results, in addition to what has been found[3] in II-VI

TABLE II. The parameters σ_0, phonon energy $h\nu_p$ associated with Urbach tails, the adjustable parameter X of Eq. (3), and P and N of Eq. (7) of $CuInSe_2$ samples of the present work, those reported in Refs. 10 and 16, and also of $CuInTe_2$ of Ref. 12. The estimated error is ± 0.01 in σ_0, ± 0.2 meV in $h\nu_p$, ± 0.04 in X, ± 0.01 in P and ± 0.02 in N.

Samples	σ_o	$h\nu_p$ (meV)	X	P	N
CIS40[a]	0.93	35.3	0.62	1.01	0.79
CIS650[a]	1.21	44.7	1.08	1.69	0.64
CIS700[a]	1.49	54.6	1.44	2.28	0.57
CIS750[a]	1.09	60.6	1.98	2.94	0.42
CIS1 ($x=0.053$)[b]	1.70	50.0	1.43	2.17	0.53
CIS2 ($x=0.047$)[b]	1.90	49.3	1.39	2.12	0.54
CIS3 ($x=0.026$)[b]	2.20	46.0	1.22	1.88	0.58
CIS4 ($x=0.020$)[b]	2.33	44.0	1.12	1.74	0.61
CIS5 ($x=-0.017$)[b]	2.75	38.5	1.39	1.35	0.68
CIS6 ($x=-0.026$)[b]	2.85	38.0	0.83	1.31	0.69
CIS7 ($x=-0.052$)[b]	2.70	36.0	0.74	1.18	0.72
CIS8 ($x=-0.150$)[b]	2.80	41.5	0.99	1.56	0.64
CIS9 ($R=0.92$)[c]	1.78	57.0	1.82	2.70	0.44
CIS10 ($R=1.02$)[c]	3.76	35.0	0.69	1.11	0.73
CIT530[d]	1.85	24.1	0.40	0.57	0.88
CIT590[d]	1.64	33.6	0.79	1.28	0.72
CIT690[d]	1.71	22.6	0.24	0.40	0.90
CITVB[d]	1.55	30.8	0.58	0.96	0.81

[a] Present work.
[b] Reference 10.
[c] Reference 16.
[d] Reference 12.

compounds, indicate that longitudinal or transverse optical phonon modes are not exclusively involved in the electron–exciton-phonon interaction just below the band edge.

It is thus proposed that the wide range of $h\nu_p$ observed in different samples of the same semiconductors in general, and in the ternary compounds in particular, could be related to their defect chemistry. These defects are probably due to structural disorder caused by the deviation from the ideal stoichiometry 1:1:2 in CIS and CIT and 1:3:5 in $CuIn_3Se_5$ and $CuGa_3Se_5$. This deviation is due to the very different vapor pressures of the constituent elements, in particular that of selenium, which is about 6 times higher than that of copper and indium at a given temperature.[17] This leads to the volatilization and loss of elemental selenium during crystal growth, causing the formation, in general, of cation and anion vacancies and interstitials and cation-cation disorder. Zhang *et al.*[27] have reported in an extensive study, the low formation energies of Cu vacancies (partly responsible for *p*-type self-doping), substitutions of In by Cu, and in particular, the formation of low-energy defect pairs. Similar phenomena exist for $CuInTe_2$.

Since the structural disorders in I-III-VI_2 ternary compounds are expected to be related to the deviation from ideal stoichiometry, for the analysis of the data we use the parameters $|\Delta x|$ and $|\Delta y|$ that determine the deviation from molecularity and valence stoichiometry respectively. These are defined as[12]

$$\Delta x = \frac{|A|}{|B|} - 1 \tag{5}$$

and

$$\Delta y = \frac{|C|}{|A|+|B|} - 1, \tag{6}$$

where $|A|$, $|B|$, and $|C|$ are the concentrations of the corresponding atoms in the compound.

From the compositional analysis of different samples of $CuInSe_2$ in the present work and those reported in Refs. 10 and 16, the parameters $|\Delta x|$ and $|\Delta y|$ are computed and reported in Table III. To correlate the effects of structural disorder on the phonon energy we define a parameter $|\Delta z| = |\Delta x| + |\Delta y|$ that roughly accounts for the contribution of deviations from molecularity and valence stoichiometry. The variation of $h\nu_p$ with $|\Delta z|$ is plotted in Fig. 3. Excluding the data points from samples CIS1, CIS7, and CIS8 (defined in Table III) that have more than approximately 10% deviations in molecularity, a linear fit is obtained that gives $h\nu_p = 30 \pm 5$ meV at extrapolation to $|\Delta z| = 0$ (the limit of an ideal stoichiometric sample). Such a value is very close to the highest LO mode reported in $CuInSe_2$ (29 meV), giving a reassuring consistency to our analysis. This implies that in the formation of Urbach tails, for systems with deviations from ideal stoichiometry, an additional phonon energy appears roughly linearly related to $|\Delta z|$. The argument for discarding samples CIS1, CIS7, and CIS8 is that, according to the pseudobinary phase diagram for the CuInSe system, approximately 10% or larger deviations would imply the existence of a secondary phase.[28,29] Thus the values of Δz reported here do indeed represent strong disorders within the studied phase.

The variation of $E_U = KT/\sigma$ against T of $CuInSe_2$ samples CIS650, CIS700, CIS750, and CIS40, shown in Fig. 4, was compared to Eq. (3) with $\Theta = 166.5$ K (Ref. 30) (Debye temperature $\Theta_D = 222$ K) using the temperature-independent structural disorder parameter X proposed by Cody *et al.* The best fits, shown by the solid lines, were obtained with the X values given in Table II. The experimental variation of E_U with T of the samples studied by Shioda *et al.* and Nakanishi *et al.* was also analyzed. The data were obtained by first calculating σ versus T from Eq. (2) for each sample, from σ_0 versus $h\nu_p$ data of Fig. 6 in Ref. 10 and Fig. 3 of Ref. 16. From this, the temperature dependence of E_U was calculated. The best fit for each sample (not shown here, but similar to that of Ref. 10) was obtained with the value of X given in Table II. Since the theoretical fit is far from satisfactory, it can be asserted that the model used by Cody *et al.* for topological disorder is not applicable to semiconductors with structural defects such as those considered here. However, a trend is observed in Table II, similar to Table II of Ref. 12 for CIT, where $h\nu_p$ increases with X.

Hence, extending this observed trend and to get a better empirical estimate of E_U versus T, we propose a modified version of Eq. (3). This includes, in addition to the structural disorder term $K(\Theta/\sigma_0)X/2$, analogous to that suggested by Cody *et al.*,[15] another parameter that permits only a partial

TABLE III. The phonon energy $h\nu_p$ associated with Urbach tails, the deviation from molecularity $|\Delta x|$, and valence stoichiometry $|\Delta y|$ and $|\Delta z|=|\Delta x|+|\Delta y|$ of $CuInSe_2$ samples of the present work and those reported in Refs. 10 and 16.

Samples	$h\nu_p$ (meV)	$\lvert\Delta x\rvert+1=\frac{\lvert Cu\rvert}{\lvert In\rvert}$	$\lvert\Delta y\rvert+1=\frac{\lvert Se\rvert}{\lvert In\rvert+\lvert Cu\rvert}$	$\lvert\Delta z\rvert=\lvert\Delta x\rvert+\lvert\Delta y\rvert$
CIS40[a]	35.3	1.008	0.993	0.015
CIS650[a]	44.7	0.991	1.019	0.028
CIS700[a]	54.5	0.976	0.970	0.054
CIS750[a]	60.5	1.014	0.965	0.049
CIS1[b]	50	0.899	1	0.101
CIS2[b]	49.3	0.910	1	0.09
CIS3[b]	46.3	0.949	1	0.051
CIS4[b]	44.0	0.960	1	0.04
CIS5[b]	38.5	1.035	1	0.035
CIS6[b]	37.0	1.053	1	0.053
CIS7[b]	36.0	1.110	1	0.11
CIS8[b]	41.5	1.353	1	0.353
CIS9[c]	57	0.92	1	0.08
CIS10[c]	35.0	1.02	1	0.02

[a] Present work.
[b] Reference 10.
[c] Reference 16.

contribution of the thermal term to the total energy. In other words, this term would reflect partial thermal occupancy of phonon states in the crystal. Our physical arguments for this model are the following: As pointed out by Zhang *et al.*,[27] defects such as Cu vacancies and Cu at In sites have the lowest defect formation energies. These are followed by vacancies of In and In on Cu sites that depend on the molecularity Cu/In. Since all the low-energy-cost defects lower the mass at the sites of an otherwise unchanged chalcopyrite structure, such defects produce well-known localized modes above the pure optical band.[31] This will reflect on $h\nu_p$ as an increase in the effective mode energy observed. On the other hand, these higher-energy modes have an occupation handicap at a fixed temperature which increases as more of the high-energy modes are generated by defects. According to the previous arguments we propose a new version of Eq. (3) as

$$E_U(T,P,N)=K\Theta/\sigma_0\left[\frac{1+P}{2}+\frac{N}{\exp(\Theta/T)-1}\right]. \tag{7}$$

P and N are adjustable parameters. The former parameter models the bare effect of substitutional disorder and, the latter, the handicap in the thermal weight due to the ensuing high-energy localized modes. Excellent agreement with the

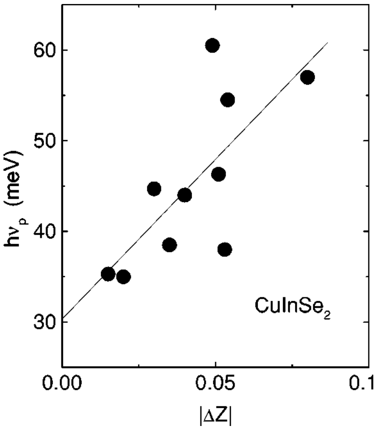

FIG. 3. Variation of the phonon energy $h\nu_p$ with the parameter $|\Delta z|=|\Delta x|+|\Delta y|$, where $|\Delta x|$ and $|\Delta y|$ are the parameters defining deviations from molecularity and valence stoichiometry.

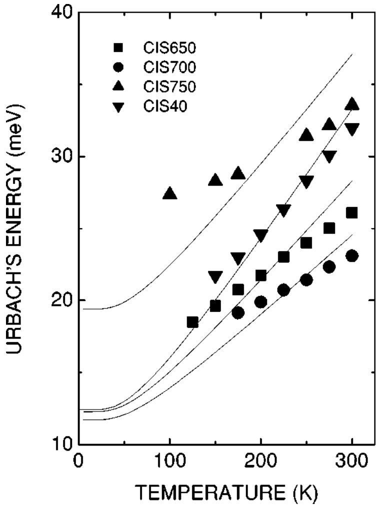

FIG. 4. The Urbach energy E_U as a function of temperature for the $CuInSe_2$ sample CIS650 (squares), CIS700 (circles), CIS750 (triangles), and CIS40 (inverted triangles). The solid curves represent a fit to Eq. (3) with the parameter X given by Table III.

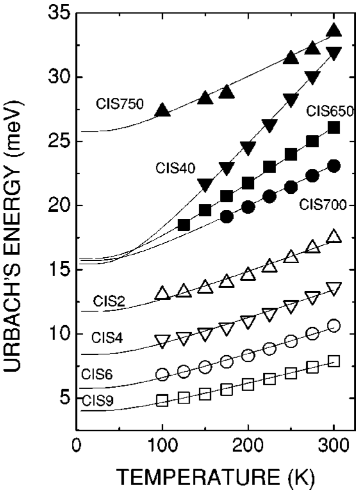

FIG. 5. The Urbach energy as a function of temperature for $CuInSe_2$ samples CIS650 (solid square), CIS 700 (solid circle), CIS 750 (solid triangle), and CIS40 (solid inverted triangle) of the present work; CIS2 (open triangle), CIS4 (open inverted triangle), and CIS6 (open circle) of Ref. 10; and CIS9 (open square) of Ref. onlineciteNakanishi. The solid curves represent a fit to Eq. (7) with the adjustable parameters P and N given in Table II.

data, as shown in Fig. 5, is obtained. The values of P and N thus estimated for all the samples are given in Table II. To further check the validity of the proposed expression, for other ternary compounds, in Fig. 6 we plot E_U versus T data of CIT samples in Ref. 12 and fit them using Eq. (7). Again, a very good fit, shown by the dashed line, is obtained for the samples termed CIT530, CIT590, CIT690, and CITVB with the parameters P and N given in Table II.

It is expected that P and N should be related to $|\Delta z|$ describing deviations from stoichiometry. To check this in Fig. 7 we plot P and N as a function of $|\Delta z|$. It is interesting that both P versus $|\Delta z|$ and N versus $|\Delta z|$ can be fitted to straight lines showing the tendency that when $|\Delta z| \rightarrow 0$ (defect free sample) P approaches zero and N to unity. In Figs. 8 and 9 we plot P and N versus $h\nu_p$ for the CIS and CIT samples, respectively. The data have been fitted to a straight line that at $P=0$ gives $h\nu_p = 20 \pm 1$ meV for CIS and 15 ± 1 meV for CIT. These values agree very well with 20 and 16 meV which are the average phonon energies of the 22 optical modes in CIS and 14 in CIT.[26] They are also not very different from their respective reported Debye temperatures which are 19 meV (221.9 K) and 17 meV (195 K).[30] Thus, these results strongly suggest that a phonon energy $h\nu_p$ higher than the average of different optical modes reported in the literature has its origin in structural disorder.

The parameter N decreases linearly with the increase of $h\nu_p$ in both CIS and CIT in Figs. 8 and 9, respectively. We emphasize that this linear behavior occurs only for devia-

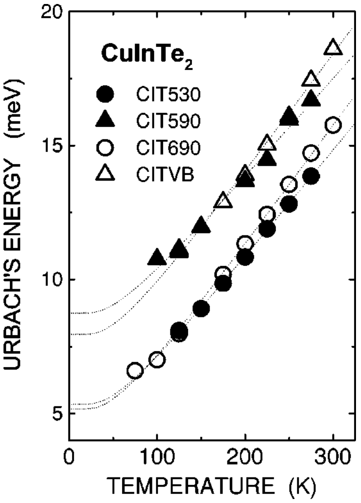

FIG. 6. The Urbach energy as a function of temperature for $CuInTe_2$ samples CIT530 (solid circle), CIT590 (solid triangle), CIT690 (open circle), and CITVB (open triangle) of Ref. 12. The dashed curves represent a fit to Eq. (7), with the adjustable parameters P and N given in Table II.

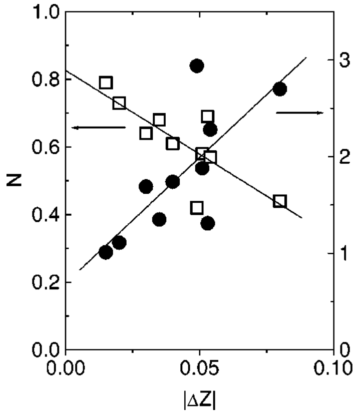

FIG. 7. Variation of the adjustable parameters P and N of Eq. (7), obtained from the fit of E_U versus T data of $CuInSe_2$ samples of the present work and of Refs. 10 and 16 with the disorder parameter $|\Delta z| = |\Delta x| + |\Delta y|$ given in Table III.

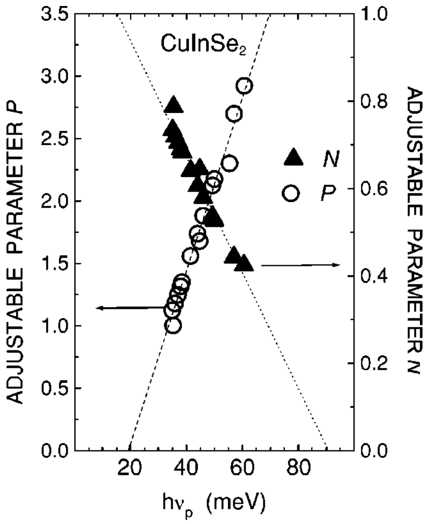

FIG. 8. Variation of the adjustable parameters P and N of Eq. (7), obtained from the fit of E_U versus T data of $CuInSe_2$ samples of the present work and of Refs. 10 and 16 with the phonon energy $h\nu_p$ associated with the Urbach tail.

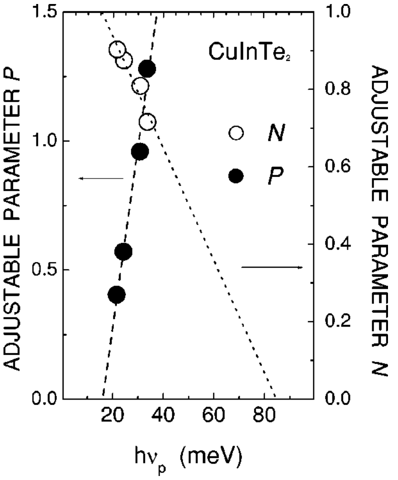

FIG. 9. Variation of the adjustable parameters P and N of Eq. (7), obtained from the fit of E_U versus T data of CuInTe$_2$ samples of Ref. 12 with the phonon energy $h\nu_p$ associated with the Urbach tail.

tions from stoichiometry of less than 10% so that $|\Delta x|$ and $|\Delta y|$ are both close to zero. Nevertheless, the extrapolation of the linear fit to $N=0$ gives $h\nu_p=91\pm 3$ meV for CIS and 85 ± 4 meV for CIT.

From the study of the pseudobinary phase diagram, it is well established[28,29] that CIS and CIT undergo a solid-state phase transition from the ordered chalcopyrite to disordered sphalerite phase at 1083 and 945 K, respectively. These temperatures correspond to 93 and 81 meV, which are very close to $h\nu_p$ of 91 and 85 meV at $N=0$ for these two compounds. This seems to imply that the maximum structural defect disorder in the chalcopyrite phase is represented by $N=0$ when an order-disorder structural phase transition is expected to occur. Extending this concept, through Eq. (7), one would expect the Urbach energy to be weakly dependent on temperature in a completely cationic disordered sphalerite phase. The intriguing relation between $h\nu_p$ and the chalcopyrite-sphalerite transition temperature deserves further theoretical study.

We should mention that, in the case of binary compounds that have only one cation and anion, large structural disorder is less likely. This is because of the high formation energy of cation-anion disorders.[32] Hence, any deviation from the ideal case $(P=0,N=1)$ is expected to be small. For this reason, the phonon energy $h\nu_p$ involved in the electron–exciton-phonon interaction in these systems is found to be close to the energy corresponding to longitudinal or transverse mode.

IV. CONCLUSION

In conclusion, the effect of structural disorder, caused by the deviation from ideal stoichiometry, on the absorption coefficient just below the fundamental edge in CuInSe$_2$ and CuInTe$_2$ was investigated. It is established that the behavior of Urbach tails in these systems is different from that reported in semiconductors with topological disorder. This behavior cannot be described in terms of the existing model of Cody *et al.* in a consistent fashion. A linear correlation is found between the additional energy in $h\nu_p$ involved in the electron–exciton-phonon interaction and the sum of the deviations from molecularity and valence stoichiometry. We interpret the additional energy in $h\nu_p$ as localized modes produced by defects above the undisturbed chalcopyrite optical bands. A two-parameter generalization of the model of Cody *et al.* is introduced to account for defects plus a term modulating the thermal weight of the localized modes. A good correlation was found between the parameters describing deviation from stoichiometry and the parameters of the proposed model giving them direct physical significance.

Strong evidence is found for our model that reproduces the correct value of $h\nu_p$ (the average phonon energy of all the lattice vibrational modes in the undisturbed structure) at zero disorder, in both CIS and CIT. The phonon energy in the fully disordered limit in each case is in good agreement with the temperature corresponding to the order-disorder structural phase transition. However, the exact physical interpretation of this correspondance at complete cation-cation disorder is still not clear. The verification of this correspondance in other materials could lead to an alternative way to identify whether they exhibit a chalcopyrite to sphalerite transition using Urbach tails. More theoretical work is needed to refine Urbach tails as an effective probe of disorder.

ACKNOWLEDGMENTS

This work was supported by grants from EEC (Contract No. Cll*-CT-92-0099 VE), CONICIT (Contract No. NM-09 and Contract No. G97-000670), and CDCHT-ULA (Contract No. 688-94-SE).

---

[1] F. Urbach, Phys. Rev. **92**, 1324 (1953).
[2] W. Martienssen, J. Phys. Chem. Solids **2**, 257 (1957).
[3] M.V. Kurik, Phys. Status Solidi A **8**, 9 (1971).
[4] H. Sumi and Y. Toyozawa, J. Phys. Soc. Jpn. **31**, 342 (1971).
[5] M. Schreiber, Phys. Rev. B **34**, 2914 (1986).
[6] B. Abay, H.S. Guder, H. Etcoglu, and Y.K. Yourtcu, Physica B **254**, 148 (1998).
[7] G. Allan, C. Delerue, and M. Lannoo, Phys. Rev. B **61**, 10 206 (2000).
[8] S. Knief and W. Von-Niessen, Phys. Rev. B **59**, 12 940 (1999).
[9] Ken-ichi Noba and Y. Kayanuma, Phys. Rev. B **60**, 4418 (1999).
[10] T. Shioda, S. Chichibu, T. Irie, H. Nakanishi, and T. Kariya, J. Appl. Phys. **80**, 1106 (1996).
[11] Y. Tang, R. Braunstein, and B. von Roedern, Appl. Phys. Lett. **63**, 2393 (1993).
[12] S.M. Wasim, G. Marín, C. Rincón, G. Sánchez Pérez, and A.E. Mora, J. Appl. Phys. **83**, 3318 (1998).
[13] S.M. Wasim, G. Marin, C. Rincon, and G. Sanchez, J. Appl. Phys. **84**, 5823 (1998).
[14] S.M. Wasim, G. Marin, C. Rincon, and G. Sanchez Perez, J. Phys. Chem. Solids **61**, 669 (2000).
[15] G.D. Cody, T. Tiedje, B. Abeles, B. Brooks, and Y. Goldstein,

Phys. Rev. Lett. **47**, 1480 (1981).

[16] H. Nakanishi, T. Sawaya, S. Endo, and T. Irie, Jpn. J. Appl. Phys., Part 1 **32-3**, 200 (1993).

[17] M.A. Arsene, A. Albacete, F. Voillot, J.P. Peyrade, A. Barra, J. Galibert, S.M. Wasim, and E. Hernández, J. Cryst. Growth **158**, 97 (1996).

[18] G. Marín, S.M. Wasim, G. Sánchez Pérez, P. Bocaranda, and A.E. Mora, J. Electron. Mater. **27**, 1351 (1998).

[19] G. Marín, C. Rincón, S.M. Wasim, C. Power, and G. Sánchez Pérez, J. Appl. Phys. **81**, 7580 (1997).

[20] V. Riede, H. Neumann, H. Sobotta, R.D. Tomlinson, E. Elliott, and L. Howart, Solid State Commun. **33**, 557 (1980).

[21] J. Gan, J. Tauc, V.G. Lambrecht, and M. Robbins, Solid State Commun. **15**, 605 (1974).

[22] H. Tanino, T. Maeda, H. Fujikake, H. Nakanishi, S. Endo, and T. Irie, Phys. Rev. B **45**, 13 323 (1992).

[23] G.A. Medvedkin, Y.V. Rud, and M.A. Tairov, Phys. Status Solidi B **144**, 809 (1987).

[24] G.D. Holah, A.A. Schenk, S. Perkowitz, and R.D. Tomlinson, Phys. Rev. B **23**, 6288 (1981).

[25] H. Neumann, W. Kissinger, R.D. Tomlinson, and N. Avgerinos, Phys. Status Solidi B **112**, K19 (1982).

[26] C. Rincon, S.M. Wasim, G. Marin, J.M. Delgado, J.R. Huntzinger, A. Zwick, and J. Galibert, Appl. Phys. Lett. **73**, 441 (1998).

[27] S.B. Zhang, Su-Huai Wei, A. Zunger, and H. K-Yoshida, Phys. Rev. B **57**, 9642 (1998).

[28] M.L. Fearheily, Sol. Cells **16**, 91 (1986).

[29] L.S. Palatnik and E.I. Rogacheva, Sov. Phys. Dokl. **12**, 503 (1967).

[30] K.J. Bachmann, F.S.L. Hsu, F.A. Thiel, and H.M. Kasper, J. Electron. Mater. **6**, 431 (1977).

[31] P. Dean, Rev. Mod. Phys. **44**, 127 (1972).

[32] J.A. van Vechten, in *Handbook on Semiconductors*, edited by S.P. Keller (North-Holland, Amsterdam, 1980), Vol. 3, p. 1.